

Eight thousand years of geomagnetic field intensity variations in the eastern Mediterranean

Agnès Genevey and Yves Gallet

Laboratoire de Paléomagnétisme, Institut de Physique du Globe de Paris, Paris, France

Jean-Claude Margueron

Ecole Pratique des Hautes Etudes, Paris, France

Received 30 October 2001; revised 11 August 2002; accepted 10 December 2002; published 2 May 2003.

[1] Twenty new intensity determinations of the ancient geomagnetic field have been obtained from groups of potsherds and brick fragments from Syria. These artifacts, archeologically well dated from ~6000 B.C. to approximately A.D. 1200, have been analyzed using the *Thellier and Thellier* [1959] method as modified by *Coe* [1967]. Intensity values have been corrected for the effects of anisotropy of thermal remanent magnetization and cooling rate. Our results indicate that field intensities were moderate in Syria from ~6000 B.C. to ~3500 B.C., with values of ~30–40 μ T. There was a significant increase in intensity by a factor of 2 from ~3500 B.C. to ~700 B.C., which was interrupted by a moderate decrease between ~2550 B.C. and ~1750 B.C. During more recent periods, our results show an intensity minimum approximately A.D. 200 and a maximum around the tenth century. Comparison with different data sets from the eastern Mediterranean and central Asia shows that geomagnetic field intensity variations were consistent at this large regional scale, at least over the last 5 millennia. *INDEX TERMS*: 1503 Geomagnetism and Paleomagnetism: Archeomagnetism; 1521 Geomagnetism and Paleomagnetism: Paleointensity; 1522 Geomagnetism and Paleomagnetism: Paleomagnetic secular variation; *KEYWORDS*: archeointensity, eastern Mediterranean, westward drift, archeology, Mesopotamia

Citation: Genevey, A., Y. Gallet, and J.-C. Margueron, Eight thousand years of geomagnetic field intensity variations in the eastern Mediterranean, *J. Geophys. Res.*, 108(B5), 2228, doi:10.1029/2001JB001612, 2003.

1. Introduction

[2] In Syria, many archeological artifacts attest to the rich civilizations that followed one another dating from the beginning of the settling process in the Middle East about 14,000 years ago. This long prehistoric and historic past has been the subject of intensive archeological research and makes Syria a favorable place to obtain detailed records of fluctuations of the Earth's magnetic field.

[3] The variations in intensity of the geomagnetic field during the last few thousand years have previously been investigated in Middle Eastern regions, in particular, in Egypt [e.g., *Aitken et al.*, 1984; *Odah et al.*, 1995; *Odah*, 1999]. Numerous intensity data were obtained from archeologically well-dated artifacts such as pottery, bricks, tiles, or furnace fragments. Unfortunately, the data sets produced by different researchers display quite different patterns of variations, which prevents the establishment of a precise and coherent intensity variation curve. These discrepancies may arise from age uncertainties, although this possibility seems rather unlikely because the chronologies used to date the artifacts were relatively well established in this archeologically rich region. They may be related also to the techniques used for intensity determination (including meth-

ods and selection criteria), since they differ from one study to another. In this study, we present new archeointensity results from 20 groups of potsherds and brick fragments collected in Syria which allow us to constrain better the evolution of geomagnetic field intensity in the Middle East during the last 8 millennia.

2. Archeological Sampling

[4] Our samples were collected from eleven different archeological sites, principally located along the Euphrates river to the east of Syria (Figure 1 and Table 1). All are made of baked clay and consist either of pottery or brick fragments. The dating of these archeological fragments is determined in two steps. The samples are first dated in a relative way since they were all found in specific occupation layers that are related to a given cultural settlement (or a civilization) from Mesopotamia or to a known episode of the regional history (for instance, the destruction of one city). This time relationship then allows their absolute dating using the chronology established for the region of interest (Table 1) [e.g., *Gothenburg Colloquium*, 1987].

[5] We only selected sample groups for which the relative dating is well constrained by the combination of several archeological arguments, such as ceramic typology, stratigraphy for multilayered sites or by the finding of age-

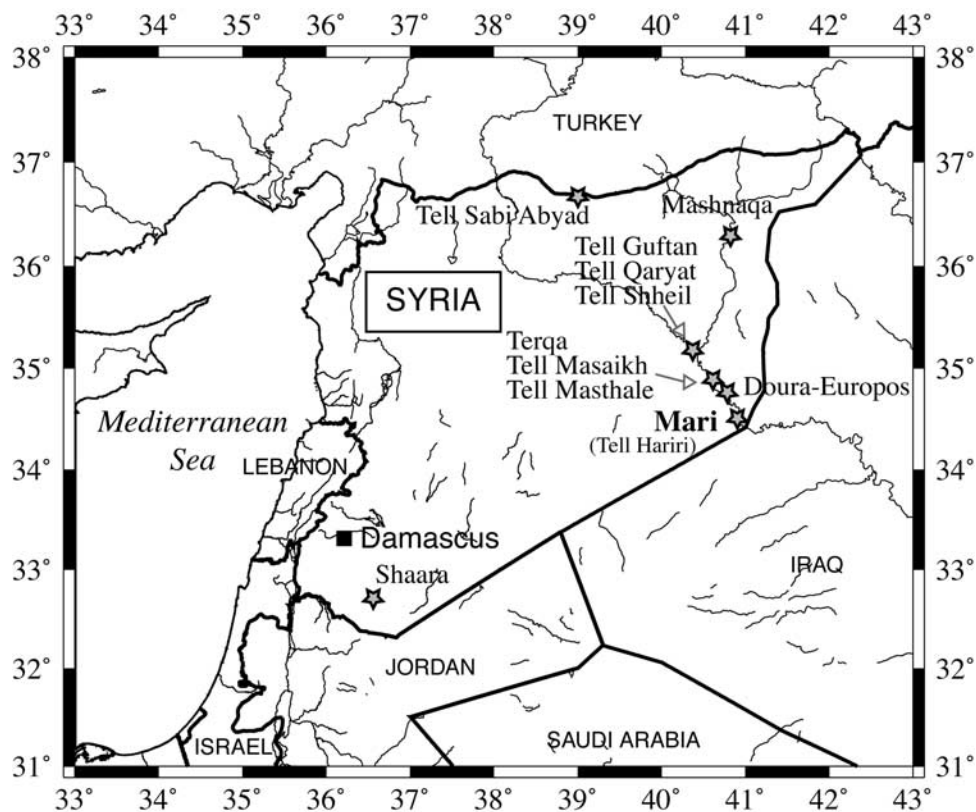


Figure 1. Location map of the different archeological sites in Syria where the groups of pottery and brick fragments were collected.

diagnostic objects (jewels, cylindrical seals, toys, etc.). In some cases, this dating is strongly ascertained by inscriptions mentioning a king name, for instance, on clay tablets or artifacts deposited in monument foundations. Among the studied sites, Mari (Tell Hariri) is of particular interest because three successive important cities occurred at this place between the third and the second millennium B.C. [e.g., Margueron, 1992; see also *Mari Annales de Recherches Interdisciplinaires*]. The last city, destroyed by the King of Babylon Hammurabi (~1760 B.C. following the middle chronology [e.g., Gothenburg Colloquium, 1987]), is the best documented by archeology, in particular with the excavation of an impressive palace and by thousands of tablets discovered in the ruins. In Mari, we collected five groups of samples associated with the end of the oldest city (here referenced as city 1) and to the beginning and the end of the two others cities (cities 2 and 3).

[6] Each studied group comprises about six to eight fragments taken from different ceramics or bricks. Much attention was paid to the temporal homogeneity of these samples. We only considered fragments found together in a clear archeological context. In particular, the brick fragments were collected from structures, pavements, or water conduits (including a cistern in Mari) that were still in place. We also preferred materials with a fine-grained clay paste, and when possible, we selected thick potsherds in order to avoid as much as possible large anisotropy effects on the thermal remanent magnetization (TRM). For the same reason, we collected preferentially the base of each pottery. Finally, we retained the samples showing no apparent trace

of re-firing, which would have induced the acquisition of a secondary magnetization.

3. Preliminary Thermomagnetic Selection Test

[7] Major failures in archeointensity experiments using thermal methods are often due to mineralogical changes induced by the heating procedure. There are different techniques for checking the stability of magnetic mineralogy upon heating. In our study, we systematically measured for all our pottery and brick samples thermal variations of the low-field susceptibility (K-T curves) using a Kappa-bridge KLY2/CS2 system. The heating curves were performed up to 550°C, which almost corresponds to the maximal temperature reached in our intensity experiments. The reversibility of the heating and cooling curves was used to select the samples for intensity experiments (Figure 2). On the basis of this criterion, very few samples were rejected, and most of these were rejected because of a large increase in susceptibility after heating (Figure 2f). This favorable behavior may principally result from the arid conditions which prevailed at our sites during the last millennia, preventing any noticeable alteration of the archeological fragments after their original firing (thus avoiding the formation of thermally unstable iron oxyhydroxides [e.g., Barbetti, et al., 1977]).

4. Rock Magnetic Properties

[8] We describe below the magnetic properties of the samples which gave reliable intensity results. These samples

Table 1. Location of the 11 Archeological Sites in Syria in This Study With the Relative and the Absolute Dating of the 20 Studied Groups of Potsherds or Brick Fragments

Archeological Sites	Lat, °N	Long, °E	Name of Groups	Nature of the Fragments ^a	Associated Culture, Period, Empire	References	Ages
Tell Sabi Abyad	36.7	39.0	LOT18	C	Pre-Halaf Halaf transition	<i>Akkermans and Le Mière</i> [1992]	[6200–5800 B.C.]
Tell Masaikh	35.0	40.6	LOT10	C	Late Halaf	<i>Rouault</i> [1998]	[5100–4500 B.C.]
Mashnaqa	36.3	40.8	LOT17	C	Late Obeid	<i>Beyer</i> [1998]	[4000–3800 B.C.]
Mashnaqa	36.3	40.8	LOT16	C	Early Uruk	<i>Beyer</i> [1998]	[3800–3600 B.C.]
Mashnaqa	36.3	40.8	LOT15	C	Middle Uruk	<i>Beyer</i> [1998]	[3600–3400 B.C.]
Mashnaqa	36.3	40.8	LOT03	C	Recent Uruk	<i>Beyer</i> [1998]	[3500–3300 B.C.]
Mari (Tell Hariri)	34.5	40.9	LOT12	C	Early Dynastic II (last occupation phase of city 1)	<i>Margueron</i> [1992]; <i>Mari Annales de Recherches Interdisciplinaires</i>	[2800–2600 B.C.]
Mari (Tell Hariri)	34.5	40.9	MR05	B	Early Dynastic III (pavement of city 2 Palace)	<i>Margueron</i> [1992]; <i>Mari Annales de Recherches Interdisciplinaires</i>	[2650–2450 B.C.]
Mari (Tell Hariri)	34.5	40.9	LOT14	C	Akkadian Empire (last occupation phase of city 2)	<i>Margueron</i> [1992]; <i>Mari Annales de Recherches Interdisciplinaires</i>	[2400–2200 B.C.]
Mari (Tell Hariri)	34.5	40.9	MR02	B	Dynasty of Ur III (cistern, contemporary with the construction of Hanun Dagan Palace, city 3)	<i>Margueron</i> [1992]; <i>Mari Annales de Recherches Interdisciplinaires</i>	[2100–1900 B.C.]
Mari (Tell Hariri)	34.5	40.9	MR11	B	Hammurabi of Babylon (destruction of the city 3 by Hammurabi of Babylon)	<i>Margueron</i> [1992]; <i>Mari Annales de Recherches Interdisciplinaires</i>	[1850–1650 B.C.]
Terqa	34.9	40.6	LOT09	C	Paleo-Babylonian period	<i>Rouault</i> [1988]	[1750–1500 B.C.]
Tell Mashtale	34.9	40.6	LOT05	C	Cassite period	<i>Rouault</i> [1988]	[1200–1100 B.C.]
Tell Masaikh	35.0	40.6	TM01	B	Neo-Assyrian Empire	<i>Masetti-Rouault</i> [2001]	[750–700 B.C.]
Doura-Europos	34.8	40.8	LOT19	C	Hellenistic period (Foundation of Doura-Europos)	<i>Leriche and Gélín</i> [1997]	[300–150 B.C.]
Doura-Europos	34.8	40.8	LOT20	C	Roman-Parthian period (destruction of Doura-Europos)	<i>Leriche and Gélín</i> [1997]	[205–235 A.D.]
Shaara	32.7	36.6	LOT35	C	Byzantin period	<i>Villeneuve</i> [1985]	[400–500 A.D.]
Tell Shheil	35.2	40.3	LOT36	C	Omayyad Dynasty	<i>Rousset</i> [2001]	[675–750 A.D.]
Tell Qaryat Medad	35.2	40.3	LOT37	C	Abbasid Dynasty	<i>Rousset</i> [2001]	[775–900 AD]
Tell Guftan	35.2	40.3	LOT41	C	Zengid period	<i>Rousset</i> [2001]	[1100–1175 A.D.]

^aC for ceramics and B for bricks.

display very homogeneous magnetic properties, regardless of the sites where they were found, of their age, or of the nature of the fragments (bricks or pottery). This homogeneity appears relatively surprising because the manufacturing processes of the studied fragments, including the firing conditions, likely varied during the period we were interested in and the origin of the clay used to make them is different.

[9] The thermomagnetic curves generally show two drops in susceptibility (Figures 2a and 2b). The first one is observed at low temperatures, between 250°C and 350°C, and the second in higher temperatures, between ~480°C and ~540°C. This feature indicates the coexistence of at least two magnetic phases with different Curie points. For some samples, the shape of the K-T curves strongly argues for a Curie point above 550°C (Figures 2c and 2d). We also performed experiments of acquisition of isothermal remanent magnetization (IRM) and measurements of hysteresis parameters for two specimens from each group using laboratory-built instruments. In all cases, the saturation is reached in fields <0.5 T (Figure 3a). Furthermore, the hysteresis loops are never constricted, which a priori indicates that our samples do not contain a mixture of grains

with different sizes or coercivity (Figures 3b and 3c) [e.g., *Roberts et al.*, 1995]. The hysteresis parameters reported in a J_r/J_s versus H_{rc}/H_c plot are essentially in the pseudo-single-domain (PSD) range, with some values in an undefined domain range (Figure 3d) [*Day et al.*, 1977]. Altogether, these properties suggest that the magnetic mineralogy of our samples is dominated by titanomagnetite with different titanium contents. The presence of a small fraction of hematite appears unlikely, although this mineral has been reported in other archeomagnetic studies [e.g., *Odah et al.*, 1995; *Evans and Jiang*, 1996; *Chauvin et al.*, 2000; *Genevey and Gallet*, 2002].

5. Archeointensity Analyses

5.1. Procedure for Raw Intensity Measurements

[10] Among the fragments showing almost reversible thermomagnetic curves, we retained four to six fragments per group. Three cubic specimens were prepared from each samples, two for intensity studies and one for cooling rate experiments. The base of the cubes is 1 cm² with a height equal to 1 cm for the specimens taken from bricks or variable (<1 cm) for those collected from potsherds. An

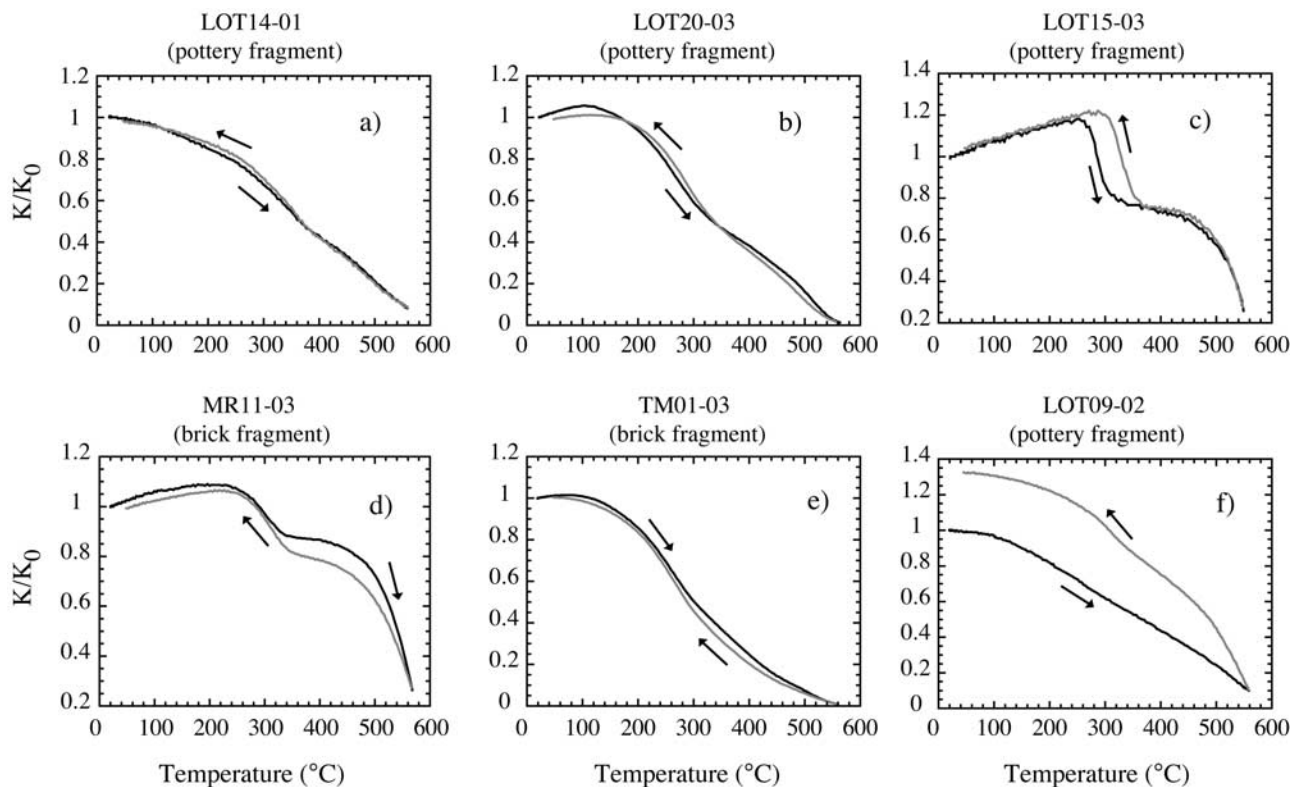


Figure 2. Normalized bulk susceptibility versus temperature curves obtained for different pottery and brick fragments. (a)–(e) Examples of favorable behavior for archeointensity determinations. (f) Example of one rejected sample because of nonreversibility of the heating and cooling curves.

arbitrary coordinate system was considered for specimen in such a way that for pottery specimens the z axis is perpendicular to the plane of the ceramics.

[11] We used the *Thellier and Thellier* [1959] method modified by *Coe* [1967] carrying out all experiments in air. The specimens were heated for 30 min and then left cooling for another 30 min. Magnetization measurements were performed using a 2G three-axis cryogenic magnetometer in the shielded room of the Institut de Physique du Globe de Paris (IPGP) laboratory. The measurement procedure involves two heating-cooling steps at each temperature, the first in a known laboratory field (H_{lab}) and the second in zero field. The first step thus induces the acquisition of a partial thermal remanent magnetization (pTRM) replacing a part of the natural remanent magnetization (NRM), and the second step causes the demagnetization of the remanent magnetization up to the considered temperature. Fourteen double heating-cooling steps were carried out from 100°C to 500°C with a temperature interval of 50°C between 100°C and 250°C and 25°C above. Every two temperature steps, pTRM checks were also made in order to detect any significant alteration of the magnetic mineralogy during heating.

5.2. Anisotropy of TRM

[12] TRM anisotropy is commonly observed in baked-clay artifacts, in particular, in pottery and bricks [e.g., *Rogers et al.*, 1979; *Aitken et al.*, 1981; *Veitch et al.*, 1984; *Chauvin et al.*, 2000; *Genevey and Gallet*, 2002] and is generally interpreted as being induced by the man-

ufacturing process. In our study, this effect was carefully estimated for each fragment because the pTRMs were not acquired in the direction of the ancient magnetization (relative to the samples). Partial TRMs measured successively in six different directions (i.e., $-x$, x , y , $-y$, z , $-z$) allowed the determination of the TRM tensor from which we computed a correction factor f [*Veitch et al.*, 1984]. These tensors were determined at two different temperatures (usually 350°C and 450°C), at which level more than 40–50% of the NRM was removed. The difference obtained for each specimen between the two correction factors is relatively small (<2% for ~70% of the samples and in all cases <6%), which fails to confirm the temperature dependence of TRM anisotropy proposed by *Aitken et al.* [1981] from the study of a few potsherds. We then used the mean of the two anisotropy correction factors to adjust the raw intensity values. We note that the mean factors obtained for the two specimens from each fragment are in very good agreement (differences <1.5%) which argues for a homogenous stretching of the clay paste at the fragment level.

[13] The mean TRM anisotropy correction factors are reported in Figure 4a. For pottery specimens the values are rather dispersed ranging from 0.87 to 1.21. For brick specimens the anisotropy correction is generally less important with factors clustered between 0.98 and 1.02 for ~70% of the specimens. Moreover, the comparison between the TRM anisotropy degrees (K_{max}/K_{min}) computed for the brick and pottery specimens shows that the magnetic fabric is significantly less anisotropic in bricks (Figure 4b) [*Jordanova et al.*, 1995]. This probably reflects the fact that the

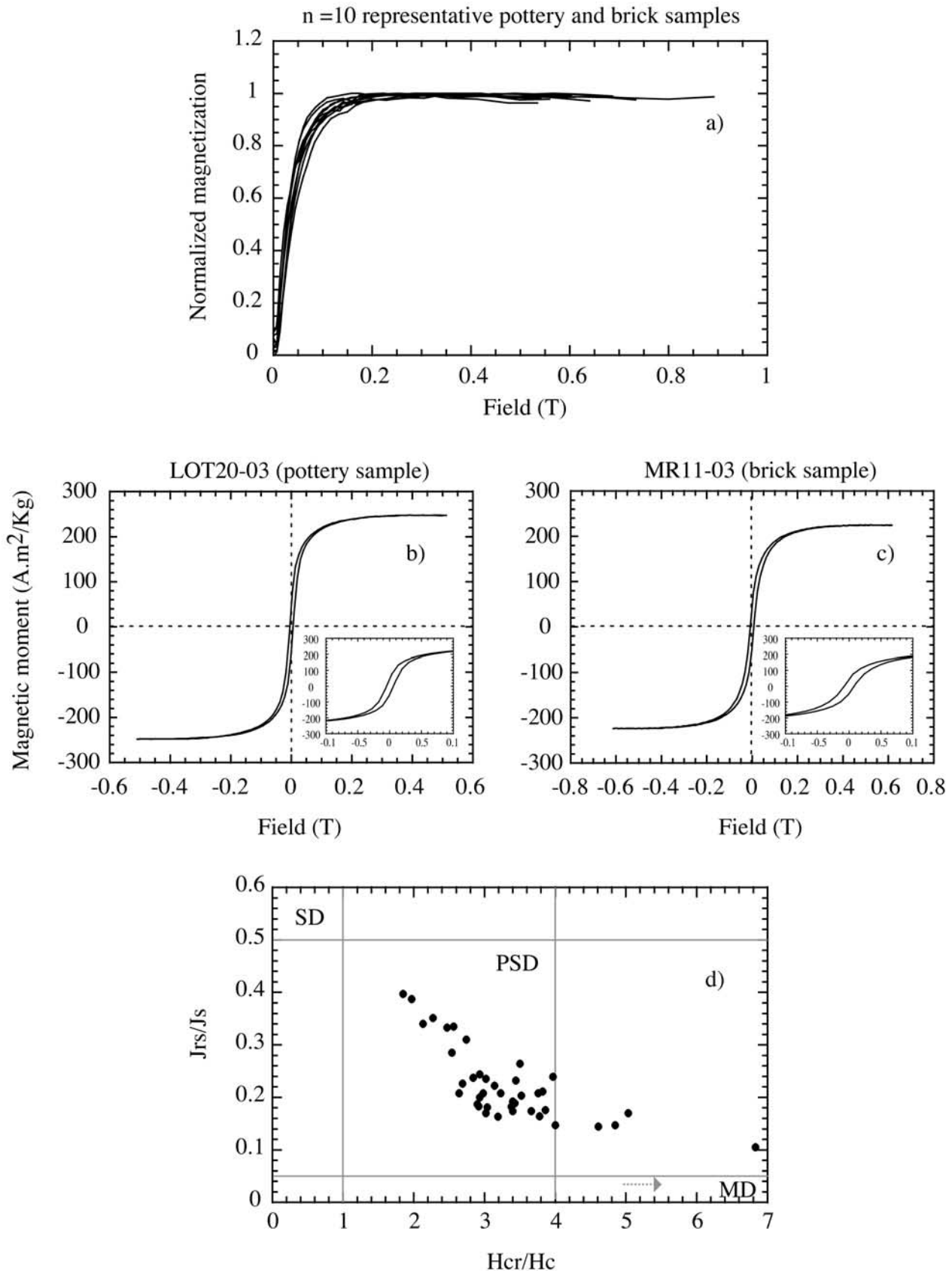


Figure 3. Rock magnetic properties of fragments which provided suitable intensity results. (a) Normalized IRM acquisition curves obtained for 10 representative pottery and brick samples. Examples of hysteresis loops obtained from (b) one pottery and (c) one brick sample. (d) Hysteresis parameters obtained from two samples from each group reported in a J_{rs}/J_s versus H_{cr}/H_c plot.

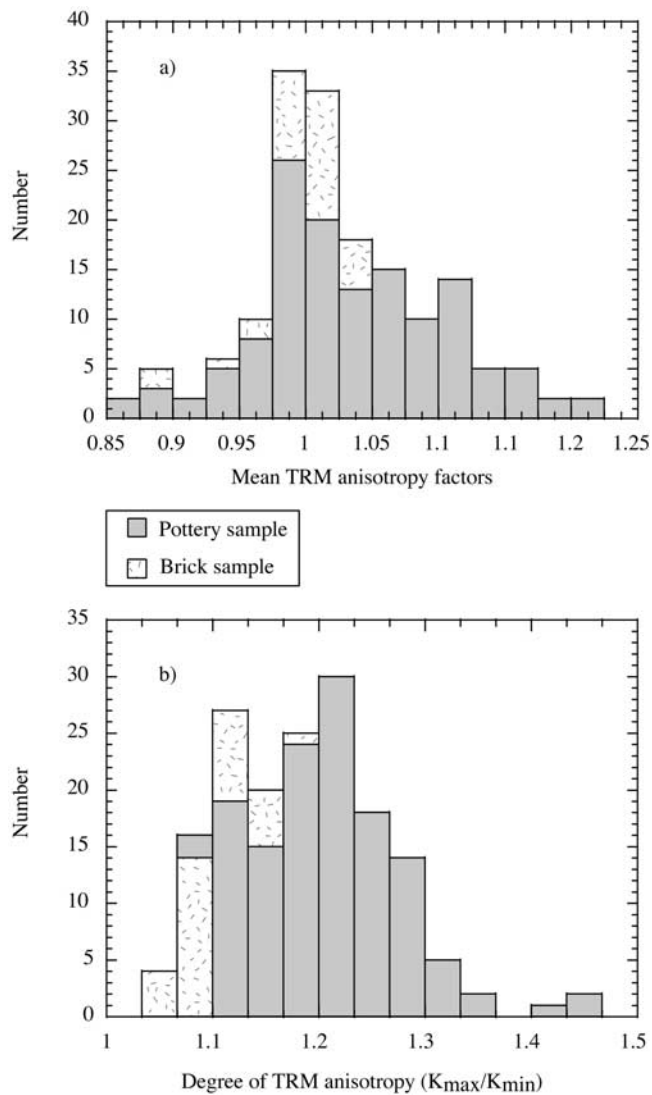


Figure 4. (a) Histogram of the mean TRM anisotropy factors and (b) histogram of the mean TRM anisotropy degrees (K_{\max}/K_{\min}) obtained for all potsherds and brick fragments.

clay paste does not suffer the same stretching constraints during brick and ceramic manufacturing.

[14] Since the chosen coordinate system of the pottery samples is related to the shape of the pottery (the z axis is perpendicular to the plane of the pottery), it is also of interest to examine the directions of the TRM anisotropy tensors. Only a few samples exhibit an anisotropy for which the principal directions are not simply linked to the pottery form [see also Aitken *et al.*, 1981; Chauvin *et al.*, 2000; Genevey and Gallet, 2002]. For most samples (~80%) the directions of the hard magnetization are almost perpendicular to the pottery planes, while the soft and intermediate directions are aligned in those planes, which is in agreement with the model of an easy plane of magnetization widely considered in archeomagnetism.

5.3. Cooling Rate Dependence of TRM

[15] The cooling rate effect on TRM acquisition is a critical parameter for archeointensity determinations [e.g.,

Fox and Aitken, 1980]. Its evaluation is based on the comparison between two TRMs acquired at the same temperature using successively a rapid and a slow cooling rate. The rapid cooling rate is the one routinely applied during intensity experiments, while the slow cooling rate must be chosen as close as possible to the one which prevailed during the original firing of the studied bricks and ceramics. In our case, the fragments were found in occupation layers with no direct connection with the kiln inside of which they were baked; the choice of the slow cooling rate is therefore rather difficult. Our choice was guided by the hypothesis that the older pottery kilns had a smaller size than the most recent ones, considering the Roman period as transition. We also considered that the kilns for making bricks were large whatever their age. Following these hypotheses, we applied a slow cooling time of ~10 hours from 450°C to 20°C for the groups of potsherds older than 300 B.C. and ~30 hours for the others groups (bricks and potsherds). These parameters are reasonable, but we acknowledge that they may not be very accurate in some cases. In order to quantify the errors which may affect the intensity determinations due to this uncertainty, we estimated for each fragment the cooling rate effect induced in three slow cooling times of 5 hours, 10 hours, and 30 hours, respectively. To this end, we performed the following experiments on new samples: (1) acquisition of a first TRM (TRM_{R1}) with a rapid cooling rate (i.e., 450°C in 30 min), (2) acquisition of a TRM with a slow cooling time of ~5 hours, referred as TRM_{Sn} ($n = 1$), and (3) acquisition of a TRM with a rapid cooling time, referred as $\text{TRM}_{R(n+1)}$ ($n = 1$). Steps 2 and 3 are then repeated 2 times with slow cooling times of 10 and 30 hours successively (i.e., $n = 2, 3$).

[16] During all these experiments the alteration of the magnetic mineralogy for each slow cooling rate was controlled by the following factor:

$$\%evol_n = \frac{abs(\|\text{TRM}_{R1}\| - \|\text{TRM}_{R(n+1)}\|)}{\|\text{TRM}_{R1}\|} (n = 1, 2, 3). \quad (1)$$

When this factor was less than ~5% (see Table 2), the cooling rate correction was computed by

$$F_n = \frac{(\|\text{TRM}_{R1}\| + \|\text{TRM}_{R(n+1)}\|)}{2\|\text{TRM}_{Sn}\|} (n = 1, 2, 3). \quad (2)$$

As can be seen from Figures 5a–5c, the cooling rate effects obtained for all samples lead generally to correction factors <1, which corresponds to an overall decrease of the raw intensity values. Such behavior is widely observed in baked clay artifacts and is in agreement with the theoretical behavior computed for an assemblage of identical single domain grains of magnetite [e.g., Dodson and McClelland, 1980; Halgedhal *et al.*, 1980; Walton, 1980]. However, the behavior is opposite (i.e., factors larger than 1) for a few samples (~11%), although this cannot be explained by any noticeable difference in the magnetic properties previously investigated (see above).

[17] The mean correction factors are roughly similar at 5, 10, and 30 hours, being ~0.95 (Figures 5a–5c), which

Table 2. Selection Criteria Used in This Study for Retaining the Intensity Results and Number of Rejected Samples Due to These Criteria

Selection Criteria for Archaeointensity Determinations	Description	Number of Fragments or Groups of Fragments Which Failed the Selection Criteria
1, "Lost NRM" versus "gained TRM" diagram	a linear segment observed on the temperature range within which was isolated the primary ATR on thermal demagnetisation diagram. stability of the magnetic mineralogy during the heating procedure: maximum of 10% of evolution between pTRM and P _{trm} check.	2 fragments rejected
	for slope computation: at least 40% fraction of NRM involved at least 5 temperature steps	7 fragments rejected
2, Coherence of the intensities values obtained for each fragment	difference between the intensities values determined for two samples from the same pottery or brick fragment $\leq 5\%$	12 fragments rejected
3, Cooling rate experiments	small mineralogical alteration during cooling rate experiments; we fixed a limit of $\sim 5\%$ of evolution.	5 fragments rejected
4, For each independently dated group	at least three archaeointensity results standard deviation of the mean = 5 μT	6 fragments rejected
		2 fragments rejected 34 rejected fragments upon 108 studied fragments rate of success $\sim 69\%$

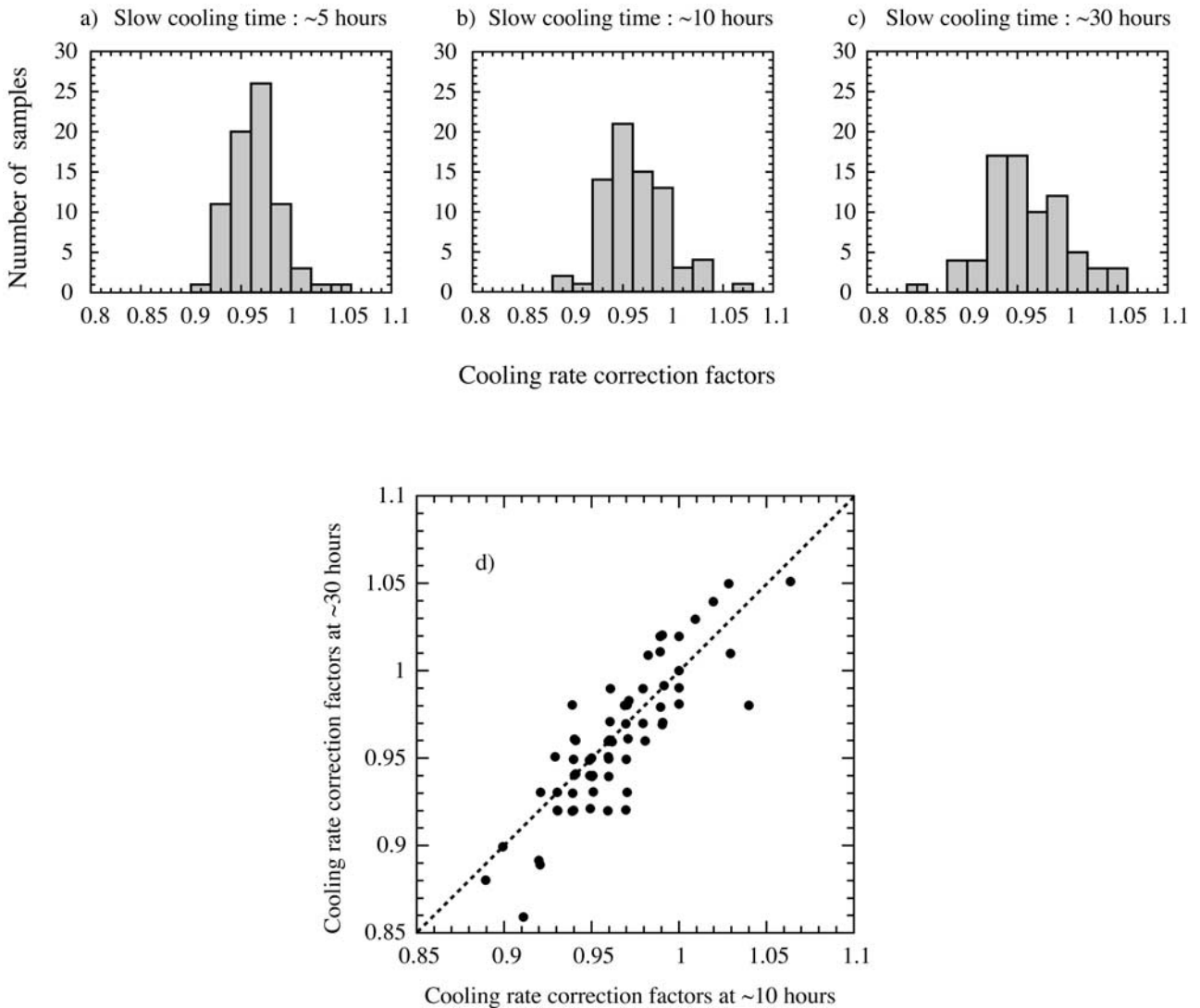


Figure 5. Analyses of the cooling rate dependence of TRM. Histograms of the cooling rate correction factors obtained for all fragments at (a) 5 hours, (b) 10 hours, and (c) 30 hours. (d) Cooling rate correction factors computed at ~ 30 hours versus those obtained at ~ 10 hours.

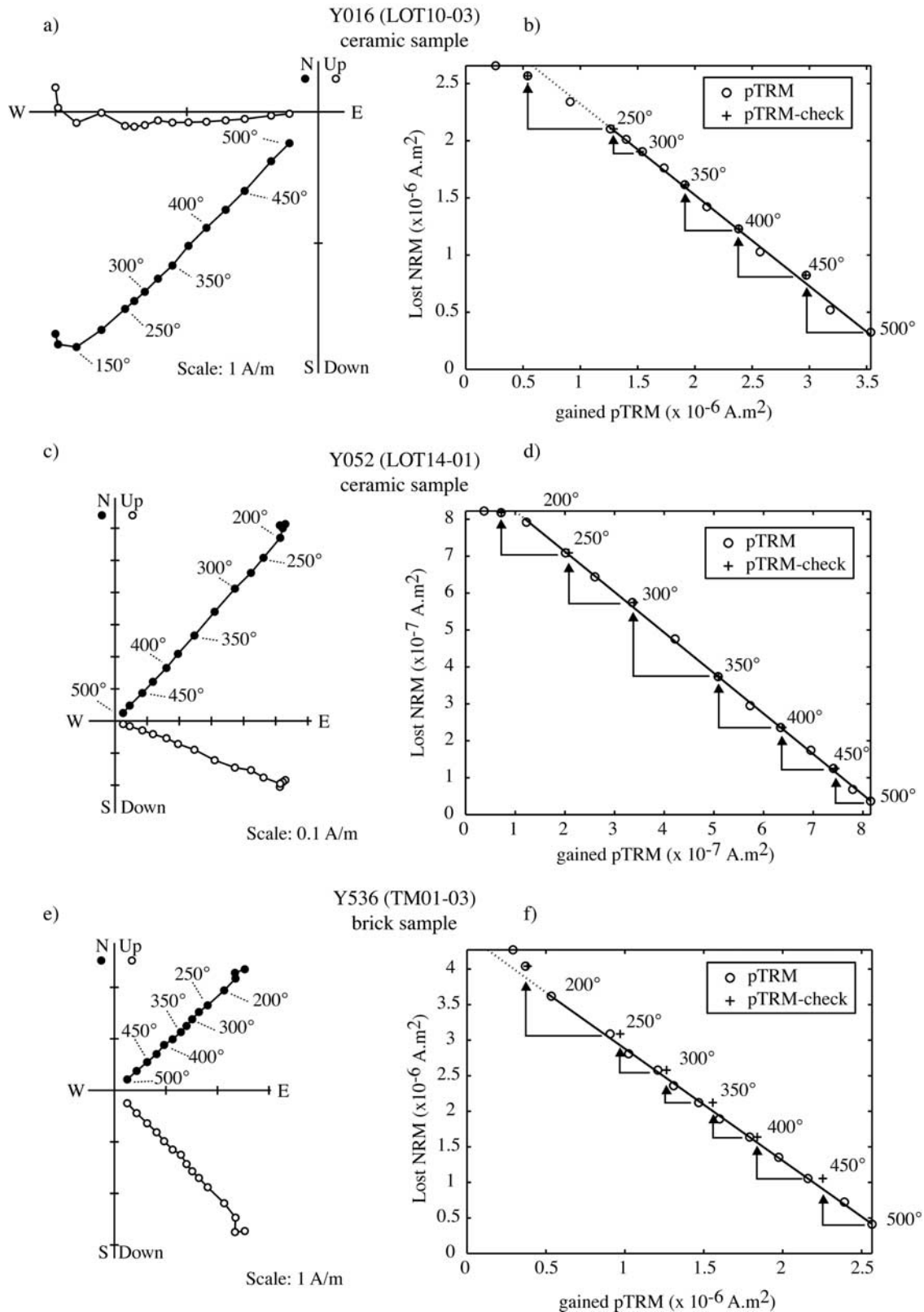


Figure 6. (a), (c), and (e) Examples of demagnetization curves and (b), (d), and (f) respective NRM/TRM diagrams. In the demagnetization diagrams, the open (solid) symbols refer to the inclinations (declinations). In the NRM/TRM diagrams, the open circles indicate the pTRM gained after each thermal step, and the crosses indicate the pTRM checks performed every two thermal steps. The linear segments considered for slope computations are indicated by a straight line within the temperature interval of determination and by dashed lines outside.

Table 3. Archeointensity Results Obtained in This Study^a

Fragments	Samples	<i>n</i>	$T_{\min}-T_{\max}$, °C	<i>f</i>	<i>g</i>	<i>q</i>	H_{lab} , μT	H_{NC} , μT	σ_H , μT	H_{AC} , μT	$H_{\text{MCRC}} \pm \Delta H$, μT	$H_{\text{mean}} \pm \sigma_H$, μT	H_{MM} , μT	VADM, × 10 ²² A m ²	$H_{\text{mean}}/H_0 \pm$ σ_H/H_0 , μT
<i>LOT18: Tell Sabi Abyad [6200–5800 BC] (2/6)^b~10 hours^c</i>															
LOT18-01	Y324	11	250–500	0.61	0.89	24.0	50	43.1	1.0	43.3	41.1 ± 0.1	40.9 ± 0.8	39.8	7.4	0.92 ± 0.02
	Y327	11	250–500	0.63	0.89	29.1	50	43.4	0.8	43.2					
LOT18-03	Y333	7	350–500	0.44	0.83	9.4	50	40.9	1.6	43.2	40.0 ± 2.1				
	Y335	5	400–500	0.33	0.75	4.3	50	36.5	2.1	39.1	(Δ <i>H</i> = 5.3%)				
LOT18-06	Y344	14	100–500	0.73	0.92	38.8	50	40.9	0.7	44.6	41.5 ± 0.1				
	Y345	14	100–500	0.74	0.92	36.4	50	39.7	0.7	44.5					
<i>LOT10: Tell Masaikh [5100–4500 BC] (3/6)^b~10 hours^c</i>															
LOT10-03	Y015	11	250–500	0.58	0.89	25.2	38	29.6	0.6	32.7	31.7 ± 0.0	32.4 ± 0.8	32.2	5.9	0.74 ± 0.02
	Y016	11	250–500	0.57	0.89	25.0	38	30.4	0.6	32.7					
LOT10-04	Y018	12	200–500	0.61	0.89	18.1	38	34.9	1.0	34.2	33.2 ± 0.4				
	Y019	11	250–500	0.60	0.88	16.2	38	35.8	1.2	34.9					
LOT10-07	Y235	11	250–500	0.62	0.89	34.3	38	35.9	0.6	34.5	32.2 ± 0.5				
	Y236	14	100–500	0.73	0.91	56.6	38	36.6	0.4	35.5					
<i>LOT17: Masnhaqa [4000–3800 BC] (3/6)^b~10 hours^c</i>															
LOT17-18	Y285	11	250–500	0.58	0.83	18.3	38	32.7	0.9	32.3	31.1 ± 0.1	31.1 ± 2.3	30.4	5.6	0.70 ± 0.05
	Y286	11	250–500	0.59	0.83	19.2	38	33.0	0.9	32.4					
LOT17-22	Y101	11	250–500	0.59	0.88	11.1	38	29.8	0.8	31.9	33.4 ± 0.5				
	Y104	11	250–500	0.54	0.88	9.7	38	29.2	1.1	30.9					
LOT17-23	Y106	11	250–500	0.47	0.89	10.4	38	28.3	0.7	28.7	28.9 ± 0.7				
	Y108	11	250–500	0.52	0.89	11.0	38	27.6	0.9	27.4					
<i>LOT16: Masnhaqa [3800–3600 BC] (3/6)^b~10 hours^c</i>															
LOT16-11	Y272	12	200–500	0.67	0.89	23.9	38	34.4	0.9	35.6	33.9 ± 0.5	33.6 ± 0.3	32.9	6.1	0.76 ± 0.01
	Y274	12	200–500	0.66	0.90	23.7	38	35.3	0.9	36.5					
LOT16-12	Y086	11	250–500	0.56	0.90	19.5	38	34.4	0.9	34.2	33.5 ± 0.1				
	Y087	11	250–500	0.55	0.90	17.5	38	34.7	1.0	34.0					
LOT16-13	Y275	13	150–500	0.75	0.90	35.4	38	35.2	0.7	34.5	33.4 ± 0.7				
	Y276	10	150–425	0.60	0.87	20.0	38	36.4	1.0	35.8					
<i>LOT15: Masnhaqa [3600–3400 BC] (3/6)^b~10 hours^c</i>															
LOT15-02	Y260	10	200–450	0.68	0.81	21.1	38	34.9	0.9	34.7	33.7 ± 0.8	33.9 ± 0.6	33.2	6.1	0.77 ± 0.01
	Y261	10	200–450	0.67	0.82	21.2	38	35.7	0.9	36.2					
LOT15-04	Y263	9	250–450	0.49	0.78	19.9	38	35.2	0.7	35.2	33.4 ± 0.4				
	Y264	9	250–450	0.49	0.79	15.6	38	33.6	0.8	34.4					
LOT15-06	Y077	12	200–500	0.84	0.90	55.1	38	32.3	0.4	34.4	34.6 ± 0.5				
	Y078	13	150–500	0.88	0.91	91.5	38	33.1	0.3	35.3					
<i>LOT03: Masnhaqa [3500–3300 BC] (3/4)^b~10 hours^c</i>															
LOT03-01	Y195	12	200–500	0.65	0.88	23.4	38	37.2	0.9	42.0	40.3 ± 0.1	40.8 ± 1.1	39.9	7.4	0.92 ± 0.02
	Y196	12	200–500	0.66	0.88	26.0	38	37.5	0.8	41.8					
LOT03-03	Y200	12	200–500	0.73	0.90	30.2	38	46.4	1.0	45.9	42.0 ± 0.2				
	Y201	12	200–500	0.72	0.90	34.2	38	44.0	0.8	46.2					
LOT03-07	Y002	12	200–500	0.50	0.88	15.5	38	40.2	1.1	43.0	40.0 ± 0.0				
	Y003	12	200–500	0.49	0.88	15.3	38	41.0	1.2	43.0					
<i>LOT12: Mari (Tell Hariri) [2800–2600 BC] (5/5)^b~10 hours^c</i>															
LOT12-02	Y040	13	150–500	0.80	0.89	52.1	38	40.9	0.6	48.1	47.6 ± 0.5	46.4 ± 1.8	46.4	8.6	1.07 ± 0.04
	Y042	13	150–500	0.78	0.89	46.9	38	44.8	0.7	49.1					
LOT12-04	Y244	13	150–500	0.66	0.91	30.6	50	46.8	0.9	48.0	46.7 ± 0.6				
	Y245	13	150–500	0.66	0.90	29.1	50	48.9	1.0	49.1					
LOT12-05	Y044	10	200–450	0.70	0.83	21.9	38	39.7	1.1	44.5	43.8 ± 0.7				
	Y045	10	200–450	0.68	0.84	26.6	38	41.7	0.9	45.9					
LOT12-06	Y048	14	100–500	0.80	0.92	55.4	50	48.7	0.6	48.4	45.7 ± 0.2				
	Y049	14	100–500	0.81	0.92	44.7	50	49.6	0.8	48.8					
LOT12-08	Y248	12	200–500	0.66	0.90	31.1	50	51.3	1.0	54.7	48.3 ± 0.5				
	Y249	12	200–500	0.66	0.90	20.2	50	48.5	1.4	53.8					
<i>MR05: Mari (Tell Hariri) [2650–2450 BC] (4/5)^b~30 hours^c</i>															
MR05-02	Y304	13	150–500	0.78	0.91	47.0	38	52.3	0.8	52.8	51.0 ± 0.9	53.0 ± 2.5	53.0	9.8	1.22 ± 0.06
	Y305	13	150–500	0.78	0.91	54.6	38	53.7	0.7	54.5					
MR05-04	Y153	13	150–500	0.80	0.91	50.4	50	61.1	0.9	57.1	56.5 ± 1.1				
	Y154	13	150–500	0.77	0.91	57.7	50	59.8	0.7	59.2					
MR05-05	Y309	13	150–500	0.74	0.91	49.5	38	53.1	0.7	55.7	52.9±0.6				
	Y310	13	150–500	0.71	0.91	40.2	38	55.8	0.9	56.9					
MR05-07	Y163	13	150–500	0.77	0.90	94.3	50	51.2	0.4	51.5	51.5 ± 0.9				
	Y164	13	150–500	0.75	0.91	62.0	50	52.1	0.6	53.2					

Table 3. (continued)

Fragments	Samples	<i>n</i>	$T_{\min}-T_{\max}$, °C	<i>f</i>	<i>g</i>	<i>q</i>	H_{lab} , μT	H_{NC} , μT	σ_H , μT	H_{AC} , μT	$H_{\text{MCRC}} \pm \Delta H$, μT	$H_{\text{mean}} \pm \sigma_H$, μT	H_{MM} , μT	VADM, × 10 ²² A m ²	$H_{\text{mean}}/H_0 \pm$ σ_H/H_0 , μT
<i>LOT14: Mari (Tell Hariri) [2400–2200 BC] (4/5)^b~10 hours^c</i>															
LOT14-01	Y052	12	200–500	0.81	0.90	100.0	50	54.8	0.4	53.8	54.9 ± 0.0	51.0 ± 2.8	51.0	9.4	1.18 ± 0.06
	Y055	12	200–500	0.80	0.90	60.3	50	53.8	0.6	53.8					
LOT14-04	Y056	13	150–500	0.81	0.90	59.9	50	49.5	0.6	53.7	49.8 ± 0.4				
	Y057	13	150–500	0.78	0.90	46.6	50	51.2	0.8	54.5					
LOT14-05	Y060	10	200–450	0.69	0.89	34.0	50	52.6	0.9	53.7	51.0±0.6				
	Y061	11	200–500	0.77	0.89	31.4	50	53.9	1.2	54.9					
LOT14-06	Y256	9	250–450	0.55	0.87	14.2	50	45.6	1.5	51.1	48.3 ± 0.3				
	Y257	9	250–450	0.56	0.87	13.1	50	46.3	1.7	51.7					
<i>MR02: Mari (Tell Hariri) [2100–1900 BC] (4/5)^b~30 hours^c</i>															
MR02-02	Y138	12	200–500	0.69	0.89	32.6	50	49.6	0.9	51.9	48.2 ± 0.2	47.9 ± 1.9	47.9	8.8	1.11 ± 0.04
	Y140	12	200–500	0.68	0.90	49.5	50	49.9	0.6	51.6					
MR02-03	Y144	13	150–500	0.75	0.91	51.2	50	51.0	0.7	53.0	50.4 ± 0.5				
	Y143	12	200–500	0.68	0.91	27.8	50	52.2	1.1	51.9					
MR02-05	Y300	12	200–500	0.71	0.91	32.1	50	47.7	1.0	47.7	46.0 ± 0.2				
	Y302	11	250–500	0.65	0.90	25.9	50	48.0	1.1	48.0					
MR02-06	Y147	13	150–500	0.77	0.89	51.1	50	47.8	0.6	49.2	46.9 ± 0.2				
	Y148	13	150–500	0.77	0.90	51.4	50	49.5	0.7	49.5					
<i>MR11: Mari (Tell Hariri) [1850–1650 BC] (3/4)^b~30 hours^c</i>															
MR11-01	Y169	10	200–450	0.71	0.86	43.2	50	41.5	0.6	42.4	40.9 ± 0.2	43.4 ± 2.2	43.4	8.0	1.00 ± 0.05
	Y170	12	200–500	0.80	0.88	59.3	50	41.4	0.5	42.0					
MR11-02	Y312	12	200–500	0.74	0.90	36.9	50	46.9	0.8	46.7	44.3 ± 0.2				
	Y313	11	150–450	0.67	0.89	28.0	50	46.0	1.0	46.4					
MR11-03	Y172	9	250–450	0.48	0.85	19.8	50	45.0	0.9	45.5	45.0 ± 0.4				
	Y175	10	200–450	0.56	0.87	29.6	50	45.5	0.8	46.2					
<i>LOT09: Terqa [1750–1500 BC] (3/6)^b~10 hours^c</i>															
LOT09-04	Y130	14	100–500	0.88	0.91	87.1	50	52.7	0.5	52.5	52.4 ± 0.1	51.0 ± 3.9	50.8	9.4	1.17 ± 0.09
	Y131	13	150–500	0.83	0.91	133.7	50	45.1	0.3	52.3					
LOT09-05	Y133	12	200–500	0.75	0.89	50.5	50	40.5	0.5	48.7	46.6 ± 0.3				
	Y134	12	200–500	0.74	0.89	41.4	50	40.8	0.6	49.3					
LOT09-08	Y222	10	275–500	0.50	0.89	14.2	38	54.5	1.7	57.5	54.1 ± 0.0				
	Y223	11	250–500	0.49	0.89	10.7	38	56.6	2.3	57.5					
<i>LOT05: Tell Masthale [1200–1100 BC] (4/6)^b~10 hours^c</i>															
LOT05-01	Y113	12	100–450	0.84	0.88	65.8	50	54.5	0.6	58.4	54.8 ± 0.6	61.5 ± 4.7	61.2	11.3	1.41 ± 0.11
	Y114	12	100–450	0.81	0.88	55.6	50	58.3	0.7	59.5					
LOT05-02	Y117	12	100–450	0.86	0.90	73.2	50	61.9	0.7	60.4	61.5 ± 0.2				
	Y118	13	150–500	0.92	0.91	66.6	50	61.0	0.8	60.1					
LOT05-05	Y207	13	150–500	0.78	0.91	51.6	50	63.4	0.9	65.0	65.0 ± 0.6				
	Y208	11	150–450	0.63	0.90	70.5	50	62.0	0.5	63.8					
LOT05-07	Y215	13	150–500	0.82	0.90	29.4	50	66.0	1.6	67.3	64.5 ± 0.6				
	Y216	13	150–500	0.76	0.91	26.8	50	65.6	1.7	68.5					
<i>TM01: Tell Masaikh [750–700 BC] (5/5)^b~30 hours^c</i>															
TM01-02	Y523	11	150–450	0.72	0.86	19.9	50	69.0	2.2	70.4	67.1 ± 0.2	71.6 ± 4.3	71.2	13.1	1.64 ± 0.10
	Y524	11	150–450	0.72	0.86	18.6	50	70.7	2.3	70.7					
TM01-03	Y527	14	100–500	0.84	0.90	35.5	50	86.1	1.8	76.6	70.3 ± 0.3				
	Y529	13	150–500	0.77	0.89	20.7	50	86.5	2.9	76.1					
TM01-05	Y536	12	200–500	0.72	0.90	65.7	50	78.7	0.8	80.3	75.6 ± 1.6				
	Y537	12	200–500	0.72	0.90	38.2	50	76.4	1.3	77.2					
TM01-06	Y540	12	200–500	0.67	0.90	22.8	50	82.4	2.2	78.7	76.6 ± 0.3				
	Y541	12	200–500	0.69	0.90	23.9	50	80.8	2.1	79.2					
TM01-07	Y543	13	150–500	0.78	0.88	29.5	50	73.3	1.7	70.4	68.5 ± 0.2				
	Y546	13	150–500	0.78	0.88	29.8	50	71.4	1.6	70.7					
<i>LOT19: Doura-Europos [300–150 BC] (3/6)^b~30 hours^c</i>															
LOT19-02	Y352	14	100–500	0.75	0.91	41.6	50	59.8	1.0	60.7	57.2 ± 1.2	57.4 ± 2.6	57.2	10.6	1.32 ± 0.06
	Y353	13	150–500	0.76	0.91	70.3	50	59.6	0.6	58.4					
LOT19-03	Y355	13	150–500	0.69	0.90	61.5	50	56.1	0.6	63.7	60.1 ± 0.4				
	Y356	13	150–500	0.67	0.90	48.2	50	55.4	0.7	62.9					
LOT19-06	Y368	12	200–500	0.54	0.87	31.9	50	51.1	0.8	57.8	55.0 ± 0.7				
	Y370	12	200–500	0.54	0.88	28.1	50	48.4	0.8	59.1					

Table 3. (continued)

Fragments	Samples	<i>n</i>	$T_{\min}-T_{\max}$, °C	<i>f</i>	<i>g</i>	<i>q</i>	H_{lab} , μT	H_{NC} , μT	σ_H , μT	H_{AC} , μT	$H_{\text{MCRRC}} \pm \Delta H$, μT	$H_{\text{mean}} \pm \sigma_H$, μT	H_{MM} , μT	VADM, × 10 ²² A m ²	$H_{\text{mean}}/H_0 \pm$ σ_H/H_0 , μT
<i>LOT20: Doura-Europos [205–235 AD] (6/6)^b~30 hours^c</i>															
LOT20-01	Y372	13	150–500	0.81	0.91	52.2	50	49.1	0.7	52.5	49.1 ± 0.3	47.1 ± 2.2	46.9	8.7	1.08 ± 0.05
	Y373	13	150–500	0.82	0.91	49.9	50	49.0	0.7	51.9					
LOT20-02	Y375	13	150–500	0.84	0.91	73.2	50	39.7	0.4	45.3	46.6 ± 1.0				
	Y376	13	150–500	0.86	0.91	124.4	50	39.6	0.2	43.4					
LOT20-03	Y380	13	150–500	0.83	0.91	64.9	50	47.9	0.6	48.2	44.2 ± 0.3				
	Y381	13	150–500	0.83	0.91	56.5	50	48.2	0.6	47.7					
LOT20-04	Y384	14	100–500	0.89	0.87	112.0	50	48.3	0.3	53.9	49.2 ± 0.4				
	Y385	14	100–500	0.89	0.87	95.8	50	48.5	0.4	53.1					
LOT20-05	Y387	12	200–500	0.71	0.91	53.3	50	52.0	0.6	52.8	48.4 ± 0.8				
	Y388	13	150–500	0.78	0.91	55.5	50	50.2	0.6	51.2					
LOT20-06	Y391	13	150–500	0.90	0.91	105.0	50	39.2	0.3	45.7	45.0 ± 0.2				
	Y392	12	200–500	0.88	0.91	91.6	50	39.4	0.3	45.3					
<i>LOT35: Shaara [400–500 AD] (4/6)^b~30 hours^c</i>															
LOT35-01	Y428	11	250–500	0.63	0.89	40.2	50	50.7	0.7	60.1	56.0 ± 0.5	55.3 ± 2.5	56.6	10.4	1.30 ± 0.06
	Y429	11	250–500	0.50	0.87	18.7	50	50.9	1.2	59.1					
LOT35-03	Y548	11	250–500	0.57	0.89	28.9	50	51.7	0.9	55.8	54.5 ± 1.0				
	Y549	11	250–500	0.55	0.88	25.4	50	53.5	1.0	57.8					
LOT35-05	Y237B	13	150–500	0.81	0.90	45.4	50	56.3	0.9	63.1	58.3 ± 0.3				
	Y239B	13	150–500	0.80	0.90	47.5	50	57.6	0.9	63.7					
LOT35-06	Y240B	13	150–500	0.61	0.90	19.3	50	53.3	1.5	52.2	52.4 ± 0.2				
	Y241B	13	150–500	0.65	0.89	23.5	50	54.4	1.3	52.5					
<i>LOT36: Tell Shheil [675–750 AD] (5/5)^b~30 hours^c</i>															
LOT36-01	Y249B	14	100–500	0.85	0.92	46.8	50	56.6	0.9	56.0	57.4 ± 0.3	56.5 ± 2.7	56.1	10.4	1.30 ± 0.06
	Y251B	13	150–500	0.81	0.91	35.6	50	57.6	1.2	56.5					
LOT36-02	Y453	14	100–500	0.89	0.90	77.4	50	54.5	0.6	55.6	56.5 ± 0.3				
	Y455	13	150–500	0.86	0.90	78.7	50	54.8	0.5	56.2					
LOT36-03	Y457	14	100–500	0.91	0.91	79.4	50	52.3	0.5	54.1	52.3 ± 0.2				
	Y458	14	100–500	0.91	0.91	67.7	50	49.5	0.6	53.7					
LOT36-04	Y460	12	200–500	0.85	0.91	58.3	50	61.3	0.8	55.1	56.9 ± 0.7				
	Y461	13	150–500	0.91	0.91	58.0	50	64.5	0.9	56.5					
LOT36-05	Y465	12	200–500	0.74	0.90	43.4	50	64.9	1.0	61.6	59.6 ± 0.5				
	Y466	12	200–500	0.73	0.90	41.2	50	65.8	1.0	62.5					
<i>LOT37: Tell Qaryat Medad [775–900 AD] (5/5)^b~30 hours^c</i>															
LOT37-01	Y468	14	100–500	0.91	0.92	77.5	50	66.4	0.7	61.1	63.2 ± 0.4	62.0 ± 2.2	61.6	11.4	1.42 ± 0.05
	Y470	14	100–500	0.91	0.92	79.7	50	65.7	0.7	60.4					
LOT37-02	Y473	12	200–500	0.76	0.90	31.6	50	61.7	1.3	61.7	61.0 ± 0.2				
	Y476	12	200–500	0.76	0.90	28.2	50	63.3	1.5	61.4					
LOT37-04	Y480	14	100–500	0.85	0.92	43.4	50	56.6	1.0	62.9	65.2 ± 1.0				
	Y481	14	100–500	0.83	0.91	29.9	50	58.4	1.5	64.8					
LOT37-05	Y484	13	150–500	0.81	0.91	60.4	50	60.6	0.7	62.4	61.0 ± 0.5				
	Y485	13	150–500	0.81	0.91	65.2	50	60.4	0.7	63.4					
LOT37-06	Y489	12	200–500	0.75	0.89	52.7	50	56.5	0.7	59.9	59.8 ± 1.1				
	Y491	12	200–500	0.73	0.90	51.0	50	56.5	0.7	62.1					
<i>LOT41: Tell Guftan [1100–1175 A.D.] (4/5)^b~30 hours^c</i>															
LOT41-02	Y494	13	150–500	0.89	0.91	145.2	50	55.0	0.3	48.4	47.0 ± 0.5	50.4 ± 3.1	50.1	9.2	1.16 ± 0.07
	Y495	13	150–500	0.89	0.91	113.3	50	54.3	0.4	47.5					
LOT41-04	Y501	14	100–500	0.81	0.92	49.9	50	58.2	0.9	56.5	54.2±0.7				
	Y502	14	100–500	0.80	0.92	48.4	50	57.2	0.9	55.2					
LOT41-05	Y504	11	250–500	0.70	0.88	45.2	50	56.4	0.8	50.2	49.1 ± 0.2				
	Y505	11	250–500	0.69	0.87	32.2	50	53.7	1.0	49.9					
LOT41-06	Y509	13	150–500	0.85	0.91	37.9	50	54.5	1.1	50.7	51.3 ± 0.1				
	Y510	13	150–500	0.82	0.90	30.7	50	55.0	1.3	50.8					

^aHere *n*, number of heating steps used to determine intensity; $T_{\min}-T_{\max}$, temperature interval of intensity determination; *f*, fraction factor; *g*, gap factor; *q*, quality factor as defined by *Coe et al.* [1978]; H_{lab} , intensity of the laboratory field; H_{NC} , noncorrected, i.e., archeointensity before TRM anisotropy and cooling rate corrections; σ_H , standard error; H_{AC} , anisotropy corrected, i.e., archeointensity after TRM anisotropy correction; H_{MV} , mean value per potsherd corrected for the cooling rate effect; $H_{\text{mean}} \pm \sigma_H$, mean intensity and standard deviation; H_{MM} , mean in Mari, i.e., mean intensity reduced to the latitude of Mari (34.5°N); VADM, virtual axial dipole moment; H_{mean}/H_0 , mean intensity normalized by the intensity at the latitude of each studied site induced by an axial dipole field with moment equal to 8×10^{22} A m².

^b nb/N , *nb* is number of fragments which fulfilled our selection criteria; *N* is number of studied fragments.

^cSlow cooling duration chosen for computing the cooling rate correction.

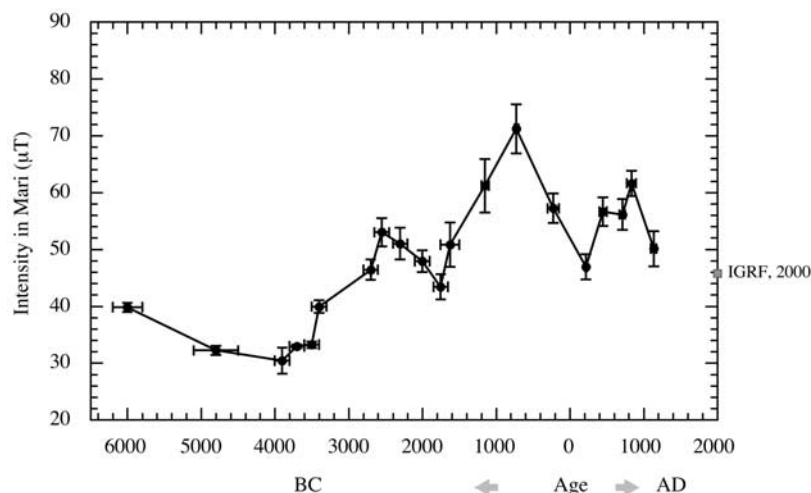


Figure 7. Evolution of the ancient geomagnetic field intensity in Syria from ~6000 B.C. to ~1200 A.D.

suggests that the choice between the three times is not critical in order to recover reliable intensity values. To confirm this observation, in Figure 5d we reported the correction factors computed at 30 hours versus those obtained at 10 hours. We note that points are distributed along the first diagonal and in all cases departures from this line are limited (<5%). This implies that if our hypotheses in choosing the value of the slow cooling rates are not fully satisfactory for some sample groups, this will not significantly change mean intensity values (we further estimated that the differences in the means between 10 and 30 hours range from -1.6% to 3.5%). The latter result is specific to this study and may depend on studied samples. The cooling rate effects observed in our Syrian samples are indeed less important than those previously obtained from French pottery with ages spanning the last two millennia and for which magnetic mineralogy was different (presence of hematite and low-Ti magnetite [Genevey and Gallet, 2002]).

5.4. Archeointensity Results

[18] The criteria used to constrain the reliability of intensity determinations have been discussed in a previous study [Genevey and Gallet, 2002] and are only summarized in Table 2. These criteria lead to the rejection of 36 samples out of 111 (Table 2), which corresponds to a quite good success rate of ~69% (recall that this success rate is reached after a selection of samples based on reversible thermomagnetic curves). Specimens were rejected for two main reasons: first, because of an unstable magnetic mineralogy upon heating (during intensity or cooling rate experiments) and, second, because of a multicomponent behavior which did not permit us to isolate the primary TRM within a sufficiently large temperature interval. The latter behavior was observed only in pottery samples which were likely refired after initial baking.

[19] Thermal demagnetizations isolate clear magnetic components above 100°C – 250°C after removal of a soft component, likely of viscous origin. Typical thermal demagnetization diagrams obtained from suitable specimens are shown in Figure 6 with their corresponding Arai plots. All intensity results including mean computations both at

the fragment and at the group levels are reported in Table 3. We point out that only one site mean value does not pass all our selection criteria (the oldest group referenced LOT18 [6200–5800 B.C.]; Table 3). The mean value is indeed computed using a fragment (LOT18-03) which failed two criteria: the NRM fraction involved for the intensity determination was too small for one of the two specimens, and the difference between the two individual intensity values was slightly larger than our 5% limit (5.5%; Tables 2 and 3). However, owing to the difficulty of obtaining such old pottery fragments, we retained this intensity value, which is otherwise very consistent with those determined from the two other fragments fulfilling the criteria.

6. Discussion

6.1. Description of Our Data

[20] The mean intensity values obtained from all our pottery and brick groups are reported in Figure 7. All results are derived at the site of Mari. We observe that the strength of the geomagnetic field was relatively moderate in Syria between ~6000 B.C. and ~3500 B.C. with values ranging from 30 to 40 μT (Figure 7). There was a significant increase in intensity by a factor of 2 from ~3500 B.C. to ~700 B.C., which was interrupted by a moderate decrease between ~2550 B.C. and ~1750 B.C. The intensity indeed reached ~71 μT during the seventh century B.C. which is ~1.6 times higher than the present intensity (45.8 μT) estimated at Mari from the international geomagnetic reference field (IGRF) model for the 2000 epoch. During more recent periods, our results exhibit an intensity minimum at around the first centuries A.D. and a maximum around the tenth century. To place these results in a larger context, it is now of interest to compare them with previous data obtained in the eastern Mediterranean.

6.2. Comparison With Intensity Results From The Near and Middle East and Greece

[21] In the last decades, many archeointensity results have been obtained from Egypt and other nearby countries from the Near and Middle East (Israel, Iraq, Cyprus [e.g.,

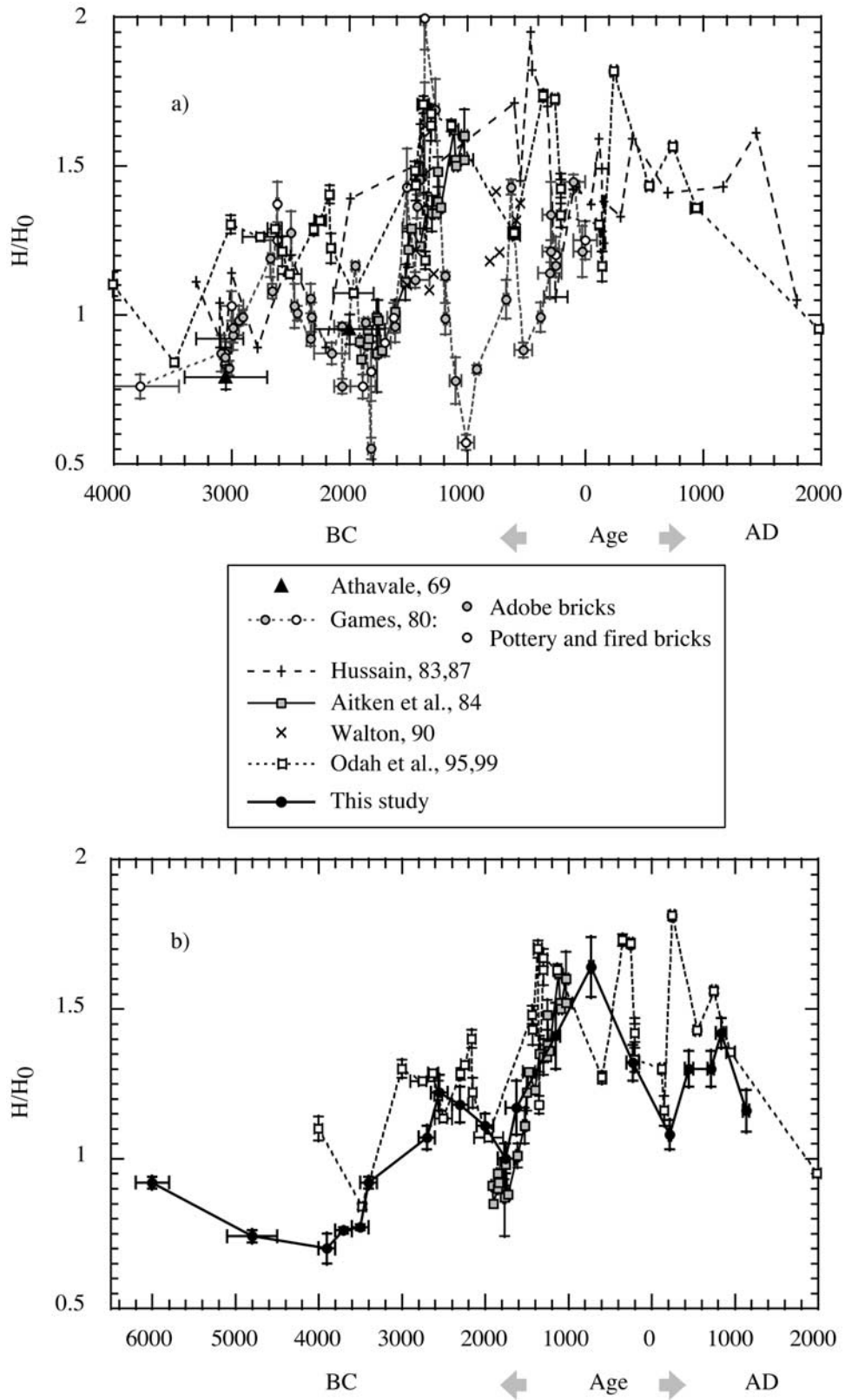


Figure 8. Intensity variations in the Near and Middle East regions. (a) Most intensity data obtained in these regions. (b) Comparison between our Syrian results and a selection of data obtained in Egypt and close countries [Aitken et al., 1984; Odah et al., 1995; Odah, 1999].

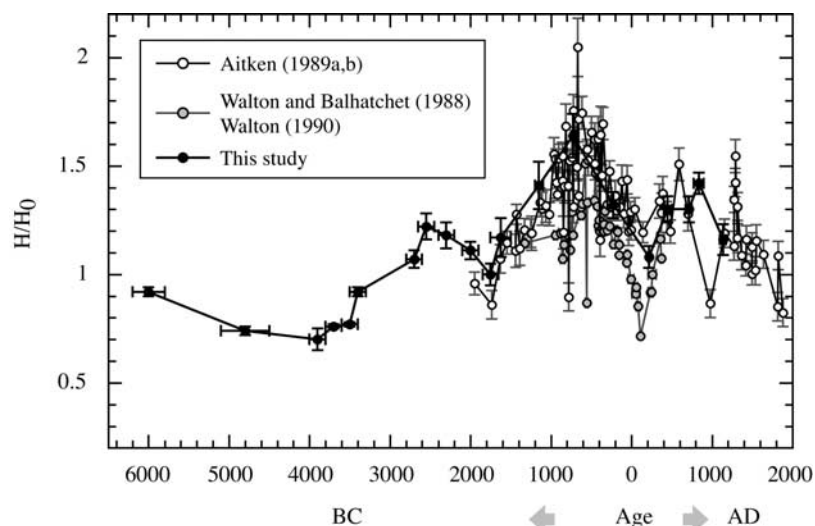


Figure 9. Comparison between the Syrian intensity results (this study) and data obtained from Greece by Aitken *et al.* [1989a, 1989b] and Walton and Balhatchet [1988] and Walton [1990].

Athavale, 1969; Games, 1980; Hussain, 1983, 1987; Aitken *et al.*, 1984; Odah *et al.*, 1995; Odah, 1999; Nachasova and Burakov, 1995]). Intensity determinations were principally made from baked clay artifacts using the *Thellier and Thellier* [1959] or the *Shaw* [1974] procedures. Games [1977, 1980] also obtained intensity results from adobe bricks using an original nonthermal method. In detail, the experimental procedures which were employed (number of samples per site, size of samples, heating and cooling time, correction or not for TRM anisotropy and cooling rate, pTRM check performed or not, etc.) and the selection criteria used to retain intensity results notably differ between these authors, which leads to an inhomogeneous collection of intensity data. For this reason, several symbols were used in Figure 8a to distinguish between data from different authors. In Figure 8a, as in the following ones,

each result is reported as the ratio of the ancient intensity to the intensity produced by an axial dipole field with the moment of the present dipole field (i.e., $8 \times 10^{22} \text{ A m}^2$) at the latitude of the studied site [Creer *et al.*, 1983]. Although we can recognize some common features, the intensity values are rather dispersed. We believe that this dispersion mainly arises from the lack of homogeneity of the data set and for this reason we will discuss below only the results which rely on the *Thellier and Thellier* [1959] methodology and selection criteria similar to ours, i.e., those obtained by Aitken *et al.* [1984] (see Aitken *et al.* [1986] for a discussion of their selection criteria) and by Odah *et al.* [1995] and Odah [1999] (Figure 8b). Very good agreement is observed between our data and those of Aitken *et al.* [1984] over the second millennium B.C., which confirms an important intensity increase at a rate of $\sim 2.5 \mu\text{T}$ per century in the

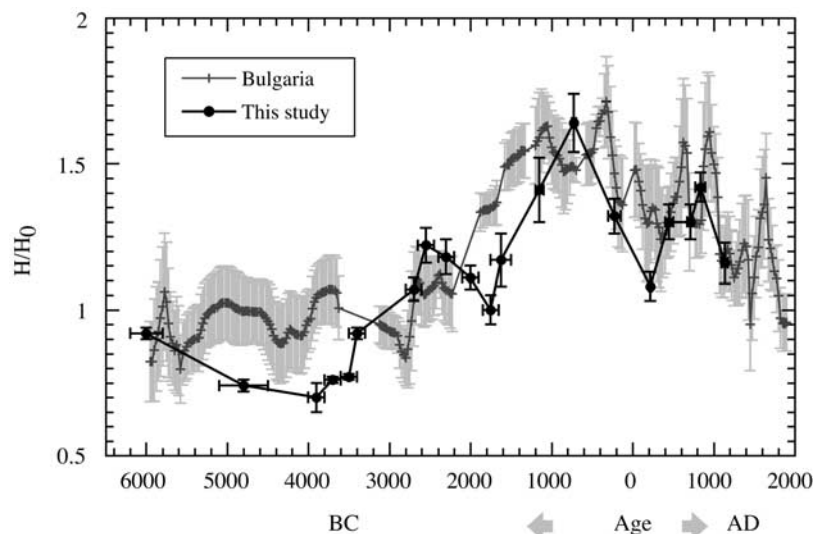


Figure 10. Comparison between the Syrian intensity results and data from Bulgaria [Kovacheva, 1997; M. Le Goff, personal communication, 2002] smoothed over 80 year-long intervals shifted every 25 years.

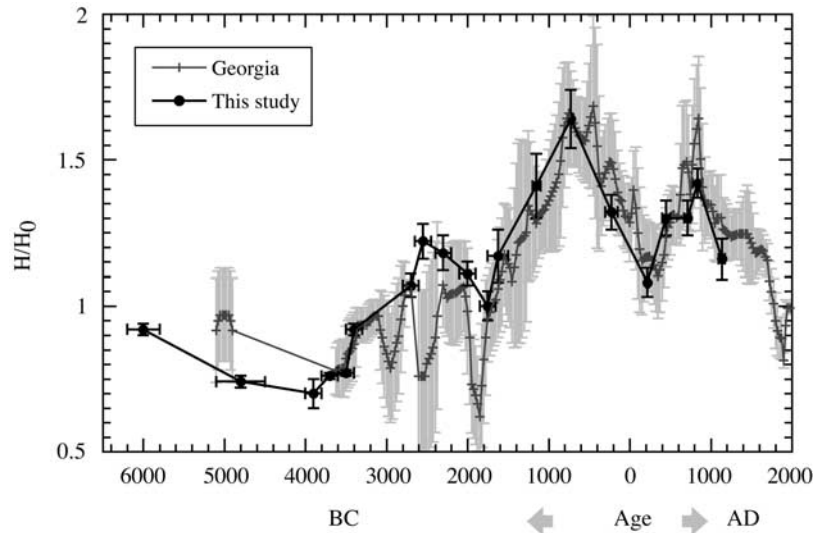


Figure 11. Intensity results from Syria and from Georgia (Caucasus [Burlastkaya, 1986; Nachasova et al., 1986; Nachasova and Burakov, 1987; Burakov and Nachasova, 1988]), the latter being smoothed over 100 year-long intervals shifted every 25 years (M. Le Goff, personal communication, 2002).

Near and the Middle East regions during this period (note that most of the data points reported by Aitken et al. [1984] correspond to the intensity value obtained from a single archeological artifact). The comparison with the Odah et al. [1995] and Odah [1999] results is more difficult: some values are consistent with ours, but their data may indicate rapid intensity fluctuations in the second millennium B.C., which neither our results nor those of Aitken et al. [1984] confirm. Some of these differences may result from the cooling rate effect which was not considered by Odah et al. [1995] and Odah [1999] and/or, in a few cases, from errors in archeological dating.

[22] Archeological samples from Greece were also the subject of several intensity studies [e.g., Liritzis and Thomas, 1980; Thomas, 1983; Papamarinopoulos, 1987; Walton and Balhatchet, 1988; Aitken et al., 1989a, 1989b;

Walton, 1990; Kovacheva et al., 2000]. Again, we decided to not compare our data with all individual data sets obtained with different intensity procedures and selection criteria but to consider the results obtained by Aitken et al. [1989a, 1989b] using almost the same criteria as applied in our studies and which describe the intensity evolution in Greece over a relatively long and continuous time interval. Figure 9 shows that they are in good concordance with our results from Syria. On Figure 9, we also report the data of Walton and Balhatchet [1988] and Walton [1990]. The latter data were obtained using a technique developed by Walton [1988a, 1988b] allowing the detection and the correction for magnetomineralogical alteration occurring during the thermal treatment. Walton indeed considered that the intensity results obtained with the Thellier and Thellier [1959] method, or variants of it, are likely systematically affected

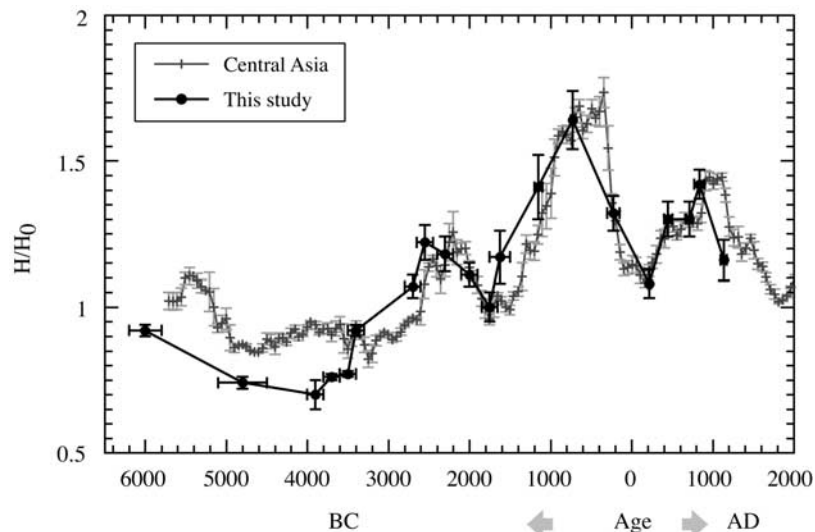


Figure 12. Comparison between data from Syria (this study) and central Asia [Nachasova and Burakov, 2000].

by alteration which leads to a lack of reproducibility and to a large dispersion of the data. In contrast, *Aitken et al.* [1986, 1988a, 1988b] argued that as long as severe selection criteria are used, these methods are reliable. We adopted this point of view after having successfully tested it on modern ceramics from France [*Genevey and Gallet*, 2002]. Moreover, the data obtained by *Aitken et al.* [1984, 1989a, 1989b] from Greece and from the Middle East are self-consistent and in very good agreement with our new data, while the data reported by *Walton and Balhatchet* [1988] and *Walton* [1990], although they exhibit the same trend in intensity between 1000 B.C. and A.D. 700, have significantly lower values (Figure 9). This further indicates the reliability of the *Thellier and Thellier* [1959] method when stringent selection criteria are applied.

6.3. Comparison With Archeointensity Data From Bulgaria and Georgia

[23] Both Bulgaria and the Caucasus region (Georgia) have seen numerous archeomagnetic investigations. In Bulgaria, numerous data were obtained during the last 30 years by M. Kovacheva and colleagues. This data set allows a complete and almost continuous description of the geomagnetic field both in direction and in intensity over the last eight millennia (see synthesis by *Kovacheva* [1997] and Figure 10). The intensity determinations were made using the classic *Thellier and Thellier* [1959] method from samples principally taken from hearths, kilns, or bricks. The TRM anisotropy effect was corrected only in recent analyses (note, however, that the anisotropy effect is weak for hearths and ovens, as shown by *Kovacheva et al.* [1998]) and estimated from the isothermal remanent magnetization anisotropy tensor [*Stephenson et al.*, 1986], whereas the cooling rate effect was considered to be <5% and was not taken into account. As a general comment, we note overall similarities between the intensity variations seen in the Bulgarian and Syrian data. However, discrepancies, marked by offsets in magnitude, are observed in the fifth and the first half of the fourth millennium B.C., and during the second millennium B.C. (which can also be described as a shift by ~500 years relative to the Syrian and Greek curves).

[24] Archeointensity analyses in Georgia were carried out by *Burlastkaya* [1986], *Nachasova et al.* [1986], *Nachasova and Burakov* [1987], and *Burakov and Nachasova* [1988]. They were principally performed on potsherds but also on bricks, tiles, and furnace fragments using a modification of the *Thellier and Thellier* [1959] method developed by *Burakov* [1981] and *Burakov and Nachasova* [1985]. This modification includes the determination of the TRM anisotropy tensor via magnetic susceptibility anisotropy assuming that the principal directions of the two tensors are the same. We note that this assumption is not always confirmed [e.g., *Garcia*, 1996]. Furthermore, no pTRM check steps were performed during the intensity determinations. Instead of pTRM checks, *Burakov and Nachasova* [1985] consider an original method to correct for chemical alteration during heating, using both a parameter called γ and changes in magnetic susceptibility during the treatment (for a detailed description of this method, see *Burakov* [1981] and *Burakov and Nachasova* [1985]). Some aspects of the method followed by these authors may be questioned, and there is

a need for intercomparison with more classical procedures. Nevertheless, when comparing their data (smoothed over 100 year-long intervals, with one point estimated every 25 years (M. Le Goff, personal communication, 2002)), an excellent concordance is observed for the last four millennia (Figure 11). The agreement is not as good for older periods: the Georgian intensity curve indeed shows rapid fluctuations which are not present in Syria.

7. Concluding Remarks

[25] Considering the very good agreement between the archeointensity data obtained from Syria (this study), Egypt and Greece [*Aitken et al.*, 1984, 1989a, 1989b], and Georgia [*Burlastkaya*, 1986; *Nachasova et al.*, 1986; *Nachasova and Burakov*, 1987; *Burakov and Nachasova*, 1988], we believe that we have established a reliable curve of the geomagnetic intensity variations in the eastern Mediterranean regions at least for the last 4 to 5 millennia.

[26] The observed fluctuations are rather smooth and do not show the rapid fluctuations with large amplitudes suggested for instance by some Egyptian data [*Odah et al.*, 1995; *Odah*, 1999] (Figure 8b). Some of these rapid fluctuations, also seen in the Bulgarian and Georgian curves, may be missing in our record because of its lower temporal resolution. However, it is worth pointing out that *Nachasova and Burakov* [2000] recently published an intensity secular variation curve for central Asia (region centered at 40°N, 65°N) spanning the last 8 millennia. This impressive curve (averaged over sliding windows of 75 years, shifted by 50 years) was established from their numerous archeomagnetic data obtained using the *Burakov* procedure [*Burakov*, 1981; *Burakov and Nachasova*, 1985] (Figure 12). The coincidence between our data and this curve is remarkable over the last 5 millennia, since the same intensity pattern is observed. This near-perfect agreement strongly argues in favor of the accuracy and the completeness of our record. For older periods (fourth and fifth millennia B.C.), however, our intensity values appear to be lower than those reported from Bulgaria [*Kovacheva*, 1997] and central Asia [*Nachasova and Burakov*, 2000]. Some Georgian data, dated from the fourth millennium B.C. show low intensity values, compatible with ours, but this is no longer the case for the fifth millennium. This intriguing point will be the subject of further studies.

[27] The above discussion shows that the Syrian archeointensity data are in very good agreement with those extending from central Europe (Greece [*Aitken et al.*, 1989a, 1989b]) to central Asia [*Nachasova and Burakov*, 2000]. In this large area, encompassing ~30° in longitude, there is thus no indication for a strong longitudinal drift of nondipole features, such as the well-known westward drift [e.g., *Evans*, 1987; *Aitken et al.*, 1989a; *Yang et al.*, 1993].

[28] Finally, we have emphasized in our study the large dispersion existing in intensity data available from different regions. However, we show that as far as stringent criteria are considered for selecting results, it is possible to isolate a coherent picture of the variations in geomagnetic field intensity.

[29] **Acknowledgments.** We are grateful to many archeologists for their help in obtaining archeological samples: Valérie Bader, Dominique

Beyer, Sophie Berthier, Hartmut Kühne, Marie Le Mière, Pierre Leriche, Béatrice Muller-Margueron, François Renel, Olivier Rouault, Maria-Grazia Masetti-Rouault, and Danièle Stordeur. We also thank Michel al Maqdisi, director of the Syrian excavation department, for helping us to work in Syria. Special thank to Vincent Courtillot and Maxime Le Goff for constructive reviews that improved the quality of the manuscript. This study was supported by IGP and CNRS. This is IGP contribution 1844 and INSU-CNRS contribution 321.

References

- Aitken, M. J., P. Alcock, G. Bussell, and C. Shaw, Archeomagnetic determination of the past geomagnetic intensity using ancient ceramics: Allowance for anisotropy, *Archeometry*, 23, 53–64, 1981.
- Aitken, M. J., A. L. Allsop, G. D. Bussell, and M. B. Winter, Geomagnetic intensity in Egypt and Western Asia during the second millennium BC, *Nature*, 310, 305–306, 1984.
- Aitken, M. J., A. L. Allsop, G. D. Bussell, and M. B. Winter, Paleointensity determination using the Thellier technique: Reliability criteria, *J. Geomagn. Geoelectr.*, 38, 1353–1363, 1986.
- Aitken, M. J., A. L. Allsop, G. D. Bussell, and M. B. Winter, Determination of the intensity of the Earth's magnetic field during archeological times: Reliability of the Thellier technique, *Rev. Geophys.*, 26, 3–12, 1988a.
- Aitken, M. J., A. L. Allsop, G. D. Bussell, and M. B. Winter, Comment on "The lack of reproducibility in experimentally determined intensities of the Earth's magnetic field," *Rev. Geophys.*, 26, 23–25, 1988b.
- Aitken, M. J., A. L. Allsop, G. D. Bussell, and M. B. Winter, Geomagnetic intensity variation during the last 4000 years, *Phys. Earth Planet. Inter.*, 56, 49–58, 1989a.
- Aitken, M. J., A. L. Allsop, G. D. Bussell, Y. Liritzis, and M. B. Winter, Geomagnetic intensity measurements using bricks from Greek churches of the first and second millennia AD, *Archeometry*, 31, 77–87, 1989b.
- Akkermans, P., and M. Le Mière, The 1988 excavations at Tell Sabi Abyad, a later Neolithic village in northern Syria, *Am. J. Archeol.*, 96, 1–22, 1992.
- Athavale, R. N., Intensity of the geomagnetic field in prehistoric Egypt, *Earth Planet. Sci. Lett.*, 6, 221–224, 1969.
- Barbetti, M., M. W. Mc Elhinny, D. J. Edwards, and P. W. Schmidt, Weathering processes in baked sediments and their effects on archeomagnetic field-intensity measurements, *Phys. Earth Planet. Inter.*, 13, 346–354, 1977.
- Beyer, D., Evolution de l'espace bâti sur un site de la vallée du Khabur au I^{er} millénaire. Les fouilles françaises de Mashnaqa, in *Natural Space, Inhabited Space in Northern Syria (10th–2nd Millennium BC)*, edited by M. Fortin and O. Aurenche, *Bull.33*, pp. 139–147, Can. Soc. for Mesopotamian Stud., Toronto, Ont., 1998.
- Burakov, K. S., Determination of the ancient geomagnetic field in magnetically anisotropic specimens, *Izv. Phys. Solid Earth, Engl. Transl.*, 17, 891–895, 1981.
- Burakov, K. S., and I. E. Nachasova, Correcting for chemical change during heating in archeomagnetic determinations of the ancient geomagnetic field intensity, *Izv. Phys. Solid Earth, Engl. Transl.*, 21, 801–803, 1985.
- Burakov, K. S., and I. E. Nachasova, Measurement of the intensity of the geomagnetic field in the territory of Georgia during the 5th–3rd millennia BC, *Geomagn. Aeron.*, Engl. Transl., 28, 900–901, 1988.
- Burlatskaya, S. P., Archeomagnetic determinations of the geomagnetic field elements, world data (in Russian), report, Geophys. Comm. of the Russ. Acad. of Sci., Moscow, 1986.
- Chauvin, A., Y. Garcia, P. Lanos, and F. Laubheimer, Paleointensity of the geomagnetic field recovered on archeomagnetic sites from France, *Phys. Earth Planet. Inter.*, 120, 111–136, 2000.
- Coe, R., The determination of paleointensities of the Earth's magnetic field with emphasis on mechanisms which could cause non-ideal behavior in Thellier's method, *J. Geomagn. Geoelectr.*, 19, 157–179, 1967.
- Coe, R., E. Grommé, and E. Mankinen, Geomagnetic paleointensities from radio-carbon-dated lava flows on Hawaii and the question of the Pacific nondipole low, *J. Geophys. Res.*, 83, 1740–1756, 1978.
- Creer, K. M., P. Tucholka, and C. E. Barton, *Geomagnetism of Baked Clay and Recent Sediments*, Elsevier Sci., New York, 1983.
- Day, R., M. D. Fuller, and V. A. Schmidt, Magnetic hysteresis properties of synthetic titanomagnetites, *Phys. Earth Planet. Inter.*, 13, 260–266, 1977.
- Dodson, M., and E. McClelland, Magnetic blocking temperatures of single domain grains during slow cooling, *J. Geophys. Res.*, 85, 2625–2637, 1980.
- Evans, M., New archeomagnetic evidence for the persistent of the geomagnetic westward drift, *J. Geomagn. Geoelectr.*, 39, 769–772, 1987.
- Evans, M. E., and L. Jiang, Magnetomineralogy of archeomagnetic materials, *J. Geomagn. Geoelectr.*, 48, 1531–1540, 1996.
- Fox, J., and M. Aitken, Cooling-rate dependence of thermoremanent magnetisation, *Nature*, 283, 462–463, 1980.
- Games, K. P., The magnitude of the paleomagnetic field: A new non-thermal, non-detrital method using sun-dried bricks, *Geophys. J. R. Astron. Soc.*, 48, 315–329, 1977.
- Games, K. P., The magnitude of the archeomagnetic field in Egypt between 3000 and 0 BC, *Geophys. J. R. Astron. Soc.*, 63, 45–56, 1980.
- Garcia, Y., Variation de l'intensité du champ magnétique en France durant les deux derniers millénaires, Ph.D. thesis 353 pp., Univ. Rennes, Rennes, France, 1996.
- Genevey, A., and Y. Gallet, Intensity of the geomagnetic field in western Europe over the past 2000 years: New data from ancient French pottery, *J. Geophys. Res.*, 107(B11), 2285, doi:10.1029/2001JB000701, 2002.
- Gothenburg Colloquium, *Acts of an International Colloquium on Absolute Chronology Held at the University of Gothenburg*, 3 vols., edited by P. Aström, Gothenburg, Sweden, 1987.
- Halgedhal, S., R. Day, and M. Fuller, The effect of the cooling rate on the intensity of weak field TRM in single domain magnetite, *J. Geophys. Res.*, 85, 3690–3698, 1980.
- Hussain, A. G., Archeomagnetic investigations in Egypt: Inclination and field intensity determinations, *J. Geophys.*, 53, 131–140, 1983.
- Hussain, A. G., The secular variation of the geomagnetic field in Egypt in the last 5000 years, *Pure Appl. Geophys.*, 125(1), 67–90, 1987.
- Jordanova, N., V. Karloukovski, and V. Spatharas, Magnetic anisotropy studies on Greek pottery and bricks, *Bulgarian Geophys. J.*, 21, 49–58, 1995.
- Kovacheva, M., Archeomagnetic database from Bulgaria, *Phys. Earth Planet. Inter.*, 102, 145–151, 1997.
- Kovacheva, M., N. Jordanova, and V. Karloukovski, Geomagnetic field variations as determined from Bulgarian Archeomagnetic data, part II, The last 8000 years, *Surv. Geophys.*, 19, 431–460, 1998.
- Kovacheva, M., V. Spatharas, and I. Liritzis, New archeointensity results from Greek materials, *Archeometry*, 42, 415–429, 2000.
- Leriche, P. and M. Gélén, *Doura-Europos études IV*, Bibliothèque Archéol. et Historique IFAO, Beyrouth, France, 1997.
- Liritzis, Y., and R. Thomas, Paleointensity and thermoluminescence measurements on Cretan kilns from 1300 to 2000 BC, *Nature*, 283, 54–55, 1980.
- Margueron, J. C., *Les Mésopotamiens*, 2 vols., A. Colin, Paris, 1992.
- Masetti-Rouault, M.-G., Rapporto preliminare degli scavi di Tell Masaikh: Il cantiere E, Athenaeum, *Studi Lett. Storia Antichità*, 89(2), 633–638, 2001.
- Nachasova, I. E., and K. S. Burakov, Change in intensity of the geomagnetic field in the second millennium BC in the territory of Georgia, *Geomagn. Aeron.*, 27, 766–768, Engl. Transl., 1987.
- Nachasova, I. E., and K. S. Burakov, Archeointensity of the geomagnetic field in the fifth millennium BC in northern Mesopotamia, *Geomagn. Aeron.*, 35(3), 398–402, Engl. Transl., 1995.
- Nachasova, I. E., and K. S. Burakov, The geomagnetic field intensity in central Asia from 6000 to 3000 B.C., *Izv. Phys. Solid Earth*, 36, 358–363, Engl. Transl., 2000.
- Nachasova, I. E., K. S. Burakov, and M. V. Kverikadze, Intensity of the geomagnetic field in the territory of Georgia to 1000 B. C., *Geomagn. Aeron.*, 26, 301–302, Engl. Transl., 1986.
- Odah, H., Improvement of the secular variation curve of the geomagnetic field in Egypt during the last 6000 years, *Earth Planets Space*, 51, 1325–1329, 1999.
- Odah, H., F. Heider, A. G. Hussain, V. Hoffmann, H. Soffel, and M. ElGamil, Paleointensity of the geomagnetic field in Egypt from 4000 BC to 150 AD using the Thellier method, *J. Geomagn. Geoelectr.*, 47, 41–58, 1995.
- Papamarinopoulos, P., Geomagnetic intensity measurements from Byzantine vases in the period between 3000 and 1650 AD, *J. Geomagn. Geoelectr.*, 39, 261–270, 1987.
- Roberts, A. P., Y. Cui, and K. L. Verosub, Wasp-waisted hysteresis loops: Mineral magnetic characteristics and discrimination of components in mixed magnetic systems, *J. Geophys. Res.*, 100, 17,909–17,924, 1995.
- Rogers, J., J. Fox, and M. Aitken, Magnetic anisotropy in ancient pottery, *Nature*, 277, 644–646, 1979.
- Rouault, O., Recherches récentes à Tell Ashara, Aboul Subartu, Studies devoted to upper Mesopotamia, edited by M. Lebeau, *Subartu*, IV(1), 313–330, 1988.
- Rouault, O., Villes, villages et steppe dans la région de Terka. Données nouvelles, in *Natural Space, Inhabited Space in Northern Syria (10th–2nd Millennium BC)*, edited by M. Fortin and O. Aurenche, *Bull.33*, pp. 191–198, Can. Soc. for Mesopotamian Stud., Toronto, Ont., 1998.
- Rousset, M.-O., La moyenne vallée de l'Euphrate d'après les sources arabes, in *Peuplement Rural et Aménagement Hydroagricoles Dans la Moyenne Vallée de l'Euphrate, fin VIIe-XIXe Siècles*, edited by S. Ber-

- thier, pp. 553–571, Inst. Fr. d'Etude Arabes de Damas, Damascus, Syria, 2001.
- Shaw, J., A new method of determining the magnitude of the paleomagnetic field, Application to five historic lavas and five archeological samples, *Geophys. J. R. Astron. Soc.*, 39, 133–141, 1974.
- Stephenson, A., S. Sadikum, and D. K. Potter, A theoretical and experiments comparison of the anisotropies of magnetic susceptibility and remanence in rocks and minerals, *Geophys. J. R. Astron. Soc.*, 84, 185–200, 1986.
- Theillier, E., and O. Theillier, Sur l'intensité du champ magnétique terrestre dans le passé historique et géologique, *Ann. Géophys.*, 15, 285–376, 1959.
- Thomas, R. C., Summary of prehistoric archeointensity data from Greece and eastern Europe, in *Geomagnetism of Baked Clays and Recent Sediments*, edited by K. M. Creer, P. Tucholka, and C. E. Barton, pp. 117–122, Elsevier Sci., New York, 1983.
- Veitch, R., I. Hedley, and J. Wagner, An investigation of the intensity of the geomagnetic field during Roman times using magnetically anisotropic bricks and tiles, *Arch. Sci. (Geneva)*, 37, 359–373, 1984.
- Villeneuve, F., L'économie rurale et la vie des campagnes dans le Hauran antique (1er siècle av. -6e siècle ap. J.-C.), in *Recherches Archéologiques sur la Syrie du Sud à l'Époque Hellénistique et Romaine*, edited by J.-M. Dentzer, 218 pp., Inst. Fr. d'Archéol. du Proche Orient, Damascus, Syria, 1985.
- Walton, D., Time-temperature relations in the magnetisation of assemblies of single domain grains, *Nature*, 286, 245–247, 1980.
- Walton, D., The lack of reproducibility in experimentally determined intensities of the Earth's magnetic field, *Rev. Geophys.*, 26, 15–22, 1988a.
- Walton, D., Comment on "Determination of the intensity of the Earth's magnetic field during archeological times: reliability of the Thellier technique," *Rev. Geophys.*, 26, 13–14, 1988b.
- Walton, D., The intensity of the geomagnetic field in the eastern Mediterranean between 1600 BC and AD 400, *J. Geomagn. Geoelectr.*, 42, 929–936, 1990.
- Walton, D., and H. Balhatchet, Application of a new techniques to Greek archeomagnetititudes, *J. Geomagn. Geoelectr.*, 40, 1503–1510, 1988.
- Yang, S., J. Shaw, and Q. Y. Wei, Tracking a non dipole geomagnetic anomaly using new archeointensity results from north-east China, *Geophys. J. Int.*, 115, 1189–1196, 1993.

Y. Gallet and A. Genevey, Laboratoire de Paléomagnétisme, Institut de Physique du Globe de Paris, 4 place Jussieu, F-75252 Paris Cedex 05, France. (gallet@ipgp.jussieu.fr; genevey@ipgp.jussieu.fr)

J.-C. Margueron, Ecole Pratique des Hautes Etudes, Section des Sciences Historiques et Philologiques (IVème section), La Sorbonne, 45–47 rue des Ecoles, 75005 Paris, France. (J_c_marg@club-internet.fr)